Modelling of Eddy Current inspections with CIVA

C. GILLES-PASCAUD, G. PICHENOT, D. PREMEL, C. REBOUD, A. SKARLATOS
CEA, LIST
91191 Gif-sur-Yvette, France
http://www-civa.cea.fr

Abstract

In the aim of fulfilling efficient ECT simulation tools within the CIVA simulation software platform, the CEA LIST has adopted several years ago a semi-analytical modelling approach. Initially limited to the simplest configurations, this approach, based on the calculation and utilization of the Green dyads, is enriched over the years with new models which, once being implemented in CIVA, allow to deal with new and more complex configurations. In this communication, after having briefly recalled theoretical aspects of the modelling approach (Volume Integral Method) we will concentrate on such recent advances. In particular examples concerning new capabilities for tubes inspection (including RFEC configurations) and multi-layered structures will be given. These examples will illustrate the simulation ability to deal with various types of probes (multi-coils, with and without ferrite, etc…). For the different cases of applications, the validity of the simulations will be evaluated by comparison with measurements.

Keywords: Eddy Currents, Simulation, Modelling, Tube inspections, Riveted structures

1. Introduction

Eddy current nondestructive testing (ECT) of conductive materials is of importance in many domains of industry: energy production (nuclear plants), transportation (aeronautic), workpiece manufacturing etc. This technique, based on the analysis of changes in the impedance of one or more coils placed near the workpiece to be tested, is used to detect and to characterize possible flaw or anomalies in the workpiece. Typical testing configurations may consist of ferrite or air core bobbin probes which are placed above a planar, layered workpiece or inside or outside a tubular workpiece and which are operated in the time-harmonic regime. The probes can as well operate in absolute mode as in differential mode with additive or subtractive flux, or in transmit-receive mode.

This contribution presents the recent progresses in developing models mainly based on the volume integral method using the Green's dyadic formalism [1] which has the capability to predict quickly the signal of an eddy current probe used in nondestructive testing. These codes form a part of the tools available in CIVA which is a powerful multi-technique (ultrasonic, radiographic, electromagnetic) platform for industrial NDT applications including a user-friendly interface. All models developed and integrated in CIVA have been validated using experimental results.

This paper is organized as follows: the semi-analytical modelling approach used in CIVA is briefly introduced in the second part. New simulation capabilities for tube inspection (including RFEC configurations) are presented in parts 3 and 4, and part 5 describes riveted structures modelling. For each case, the validation of the simulation tools is a key point, and great care has been taken for the comparison between numerical results and experimental data.

2. Introduction to the VIM approach

Semi-analytical models developed in the CIVA platform use the Volume Integral Method (VIM) based on Green's formalism [1]. The main advantages of this approach are its great accuracy, its speed, since a complete cartography is achieved with CIVA in less than an hour for a 3D ECT configuration, and the few number of numerical parameters required in the configuration description. These numerical parameters are the number of cells used to mesh the flaw and ferrite cores of the probe if any. This last point makes CIVA easier to use than purely numerical simulation tools for non-specialists in numerical analysis. The keystone of the approach consists in the solution of an integral equation [2], governing the interaction between the flaw and the primary electric field emitted by the probe in the volume containing the flaw:

$$\mathbf{J}(\mathbf{r}) = \mathbf{J}_0(\mathbf{r}) + j\,\omega\,\mu_0\,\sigma_0\,f(\mathbf{r})\int_{\Omega}\mathbf{G}(\mathbf{r},\mathbf{r}')\cdot\mathbf{J}(\mathbf{r}')\,\mathrm{d}\mathbf{r}', \tag{1}$$

where Ω is the volume of the flaw, ω is the angular frequency, $\mu_0 = 4\pi.10^{-7}$, $\mathbf{G}$ is a dyadic Green's function, σ_0 is the tube conductivity, $\mathbf{J}_0$ is an exciting term due to the probe and the function $f(\mathbf{r})$, defined by the relation,

$$f(\mathbf{r}) = \frac{\sigma_0 - \sigma(\mathbf{r})}{\sigma_0}, \tag{2}$$

This relation represents the conductivity contrast between the flawed region of conductivity $\sigma(\mathbf{r})$, and the unflawed region of conductivity σ_0. The unknown $\mathbf{J}$ is a fictitious current density defined in Ω and is determined using the Method of Moments [3]. To solve equation (1), the excitation term $\mathbf{J}_0$ has to be calculated first and is obtained from the calculation of the primary electric field emitted by the probe in the region Ω. Once the fictitious current density $\mathbf{J}$ has been calculated, ECT output signals are obtained using the reciprocity principle [4].
This modelling approach has been validated with experimental data for several industrial applications. Results presented hereafter concern tubes and fastened structures inspections.

3. EC modelling of Steam Generator Tubing Inspection

The example illustrated in Figure 1 deals with the inspection at two different frequencies of a Steam Generator tube made of Inconel (σ = 1 MS/m, μ_r = 1) affected by a transverse flaw, using a bobbin coil made of two coils operating in differential mode. The detailed characteristics of the tube, of the probe and the flaw are given in Figure 1. The scanning is performed along the axis of the tube, and simulation results are compared with experimental data in the impedance plane. A calibration procedure is applied using a through-wall cylindrical hole: once the simulation of this calibration flaw has been performed, coefficients are applied in order to fit the experimental data in terms of maximal amplitude and related phase. Those coefficients are therefore applied for any other flaws simulation. One may observe that for both frequencies simulated and experimental results agree quite well, the discrepancy being lower than 5% in amplitude and 2.5° in phase.

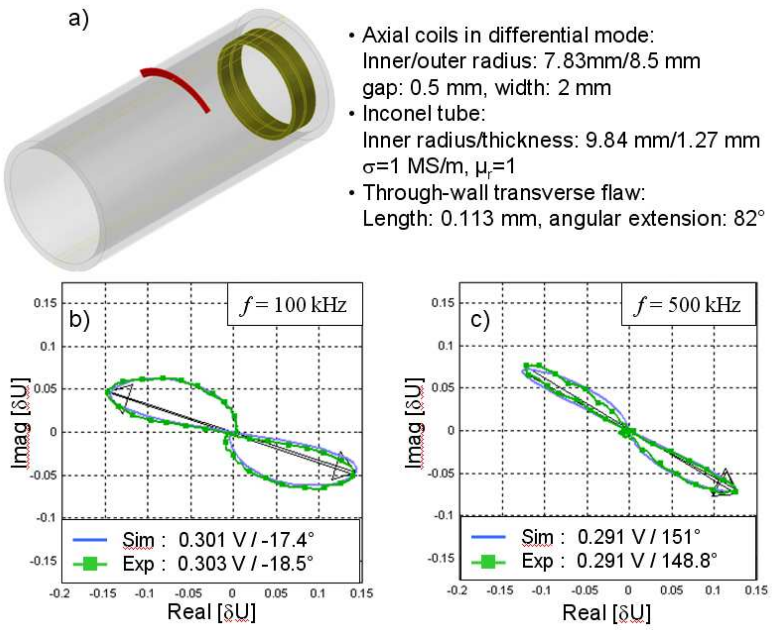

Figure 1 : Experimental and simulated ECT inspection of a transverse flaw with a bobbin coil: a) Configuration description, b) Inspection at *f* = 100 kHz, c) Inspection at *f* = 500 kHz.

Another inspection simulation has been carried out and compared to experimental data, using the same probe and the same tube, with a longitudinal flaw (Figure 2). Here again, for both frequencies simulated results and experimental data agree well, although experimental data exhibits some noise (especially at the frequency of 500 kHz, which is less favourable than lower frequencies for the detection of this external flaw). However, in spite of this noise, the agreement in amplitude and phase is better than 5% and 5°.

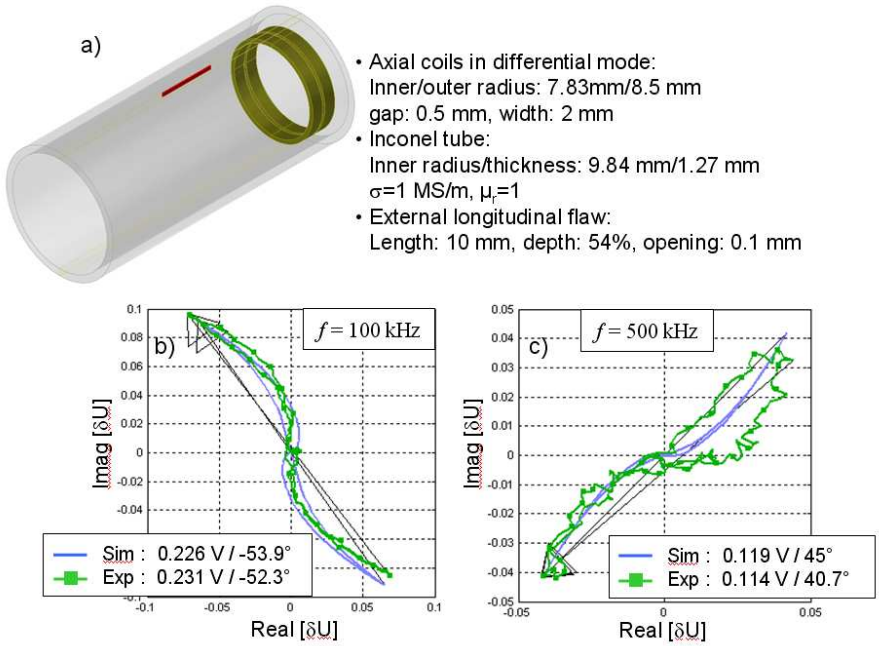

Figure 2 : Experimental and simulated ECT inspection of a longitudinal flaw with a bobbin coil: a) Description of the configuration, b) Inspection at *f* = 100 kHz, c) Inspection at *f* = 500 kHz.

The influence of probe eccentricity may also be simulated [5], as illustrated on the figure below, using two different inspection configurations for a 40% external groove: the first configuration corresponds to a centred probe (as used in the previous experimental validation examples) while, in the second configuration, the axis of the probe has been shifted by 1mm. The flaw signal is somewhat increased for the off-centred probe's case.

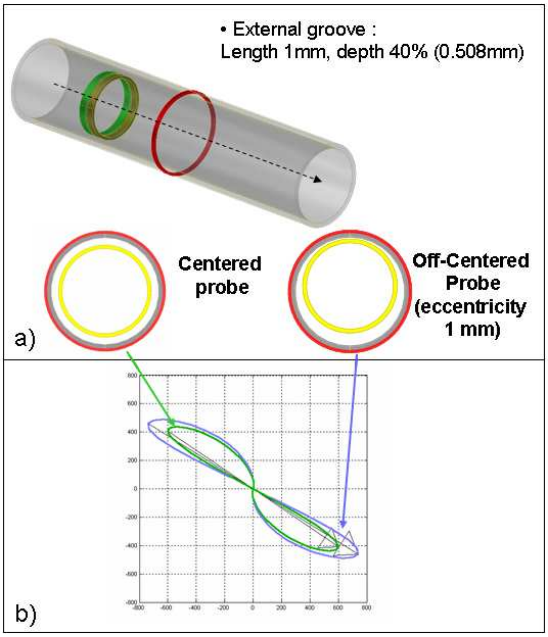

Figure 3 : Simulation of the influence of the probe's alignment over the flaw response: a) Description of the configuration, b) Simulated results at *f* = 500 kHz.

4. EC modelling of ferromagnetic tube inspection

EC testing of ferromagnetic tubes is currently applied in many industrial domains: petrol industry, nuclear energy (condensers of fast neutron reactors) or the steel production. The Remote Field Eddy Current (RFEC) technique is usually employed in such applications due to the small penetration depth inside ferromagnetic materials. The method based on the VIM formulation has been extended for the simulation of ferromagnetic tubes with specific attention given in RFEC inspection. The simultaneous local variation of both conductivity and permeability caused by material defects leads to a system of two state equations one for the electric and one for the magnetic field. The solution of this system of equations via the Method of Moments provides the electric and magnetic field distribution inside a domain containing the flaw. Finally, by applying the reciprocity theorem the variation of the eddy current signals produced by the flaw is obtained. The model, which was validated using experimental data and compared with Finite Elements Method (FEM) simulation results, is integrated into CIVA [6].

An example is given for the testing configuration described in Figure 4. This configuration takes into account a tube with an internal diameter of 14mm and an external diameter of 18mm, inspected with the RFEC technique at a frequency of 250 Hz. The conductivity and the relative permeability of the tube were measured and are equal respectively to 6.25 MS/m and 210. The probe is composed of two emitters (E1, E2), connected in additive flow, and two receivers (R1, R2) connected in differential mode.

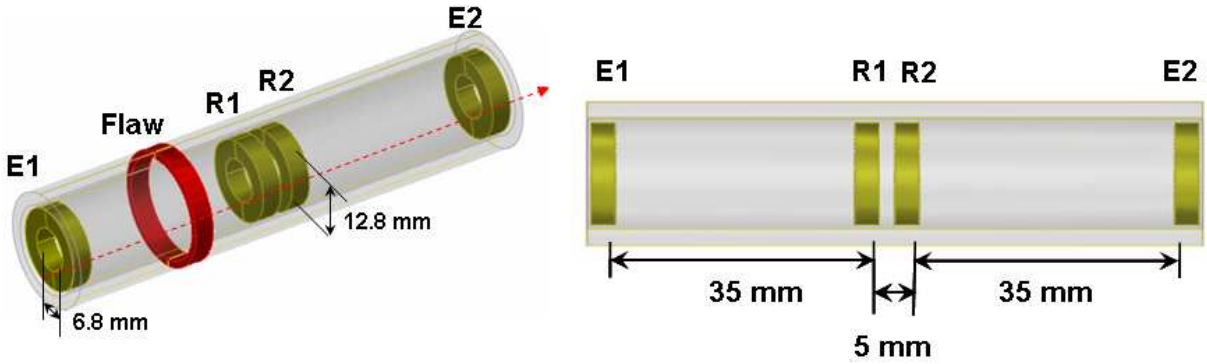

Figure 4 : Description of the Remote Field EC configuration. The dotted lines corresponds to the displacement of the probe.

Figure 5 presents the results obtained for the detection of an external groove with a 3mm width and a 20% (left part) and 70% (right part) depth. The signals were calibrated to have 5mV and 0° for the signal of an external groove with a width of 3mm and a 40% depth.

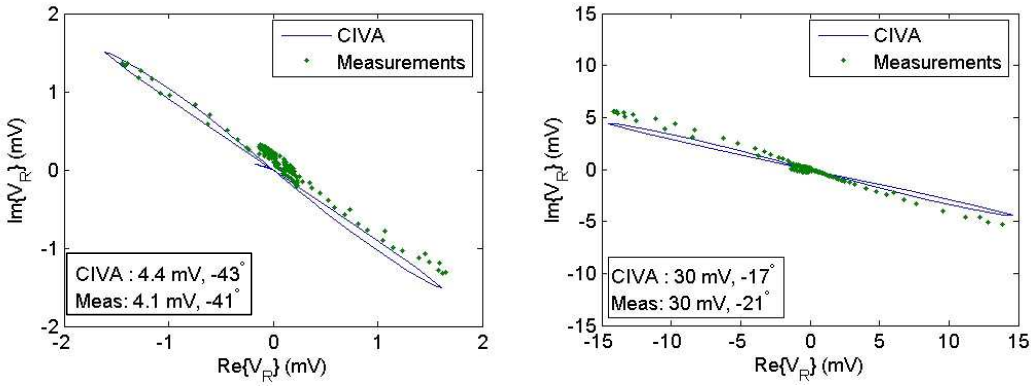

Figure 5: Simulated and experimental results obtained for an external groove of 20% (left part) and 70% (right part) depth.

Flaw	Amplitude		Phase	
	CIVA	Measure	CIVA	Measure
External groove (20%)	4.4 mV	4.1 mV	-43°	-41°
External groove (60%)	22 mV	21 mV	-21°	-24°
External groove (70%)	30 mV	30 mV	-17°	-21°

Table 1 : Comparison between experimental and simulated data.

Table 1 describes the simulated and experimental amplitude and phase values obtained for external grooves with 20% 60%, and 70% depth. These results show the good agreement between simulation and experiment for these three defects.

5. EC modelling of flawed riveted structure inspection

One of the EC testing issues in aeronautics is the inspection of fastened structures to detect flaws nearby rivets which can grow because of mechanical stress. Within the framework of a collaborative project between CEA and EADS, a simulation tool of EC fastened structures testing has been developed and integrated to the CIVA platform [7]. The whole model has been experimentally validated and compared to a Finite-Element (FE) one developed by LGEP (Laboratoire de Génie Electrique de Paris) [8]. A validation example is given for the following

configuration: 3 aluminum layers (2.5mm and 4mm thick) with a conductivity of 17 MS/m are drilled by a borehole with head diameter of 12 mm and body diameter of 6.35 mm (Figure 6). The experiments have been performed with a ferrite cored probe operating at 1.6 kHz.

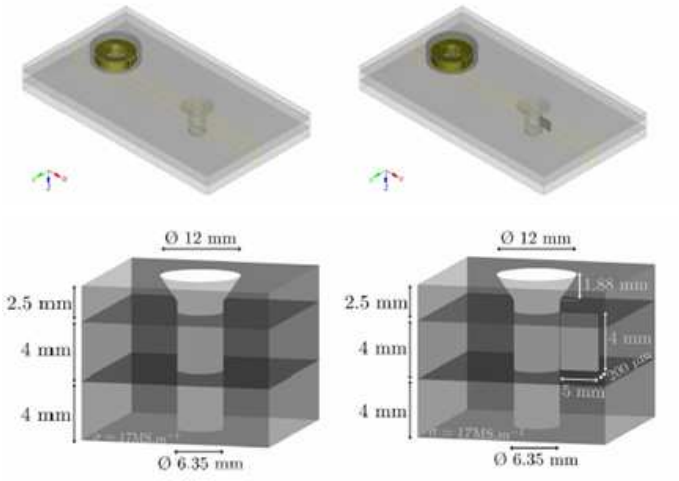

Figure 6: Configurations of studies

The issue is to cope with discrepancies of scales, the size of the rivet and the one of the flaw differing by orders of magnitude. To be sensitive to the flaw response, a calibration on the borehole configuration (left part, Figure 6) of the signals simulated versus the experimental one is seen as a preliminary step to the validation of the model. In a second step, the results obtained on a flawed configuration (right part, Figure 6) have been studied: a EDM notch was made near boreholes with a 0.2mm opening, a 5mm length and a 4mm height, and is entirely crossing the second layer.

Calibration

The experimental data as well as the data obtained with the semi-analytical model or the finite-element code have been calibrated using the EC measurement on the borehole signals in the impedance plane. Two noticeable points were used for the calibration; the first corresponds to the maximum in amplitude of the signal in the impedance plane (x=5mm) and the second is the turn back point (x=0mm) (Figure 7). We choose to calibrate the simulated signals at x = 5 mm. The Table 2 presents the amplitude and the phase values obtained at the two noticeable points. The simulated signals, after calibration, have the same amplitudes at x = 0 mm and x = 5 mm (resp. 21 mV and 29 mV) and a small phase difference of one degree.

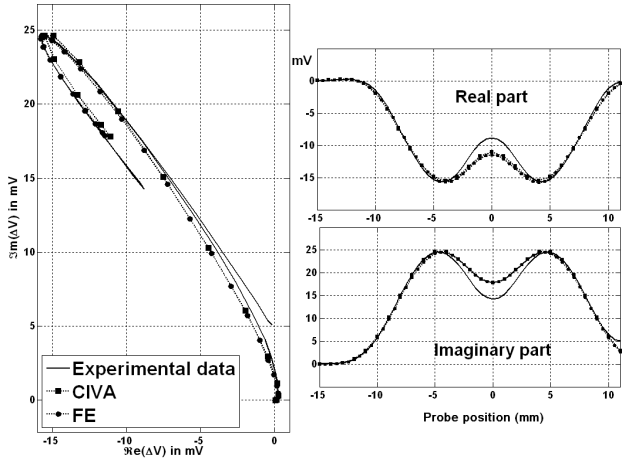

Figure 7: Calibrated signals for the borehole at 1.6 kHz.

Calibrated signals for borehole		Measures		Agreements	
		Amplitude	Phase	Amplitude	Phase
Experiment	x= 0 mm	17 mV	122°	×	×
	x= 5 mm	29 mV	123°	×	×
CIVA	x= 0 mm	21 mV	122°	24 %	0°
	x= 5 mm	29 mV	121°	0 %	2°
FE	x= 0 mm	21 mV	123°	24 %	1°
	x= 5 mm	29 mV	122°	0 %	1°

Table 2: Agreements between the calibrated signals for the borehole at f = 1.6kHz.

A good agreement between the CIVA model and the FE one is obtained (0%, 1°) at x =5 mm. Nevertheless, the two simulated signals do not accurately fit (24%, 1°) the experimental one at x = 0 mm (when the probe is placed right above the borehole). This discrepancy, which remains acceptable considering the complexity of the configuration, can be due to the 3D ferrite core (cylindrical core with slots) of the probe, not modelled with CIVA and the FE code.

Validations results with the flaw in the second layer

The signals are presented in the impedance plane (experiment and semi-analytical model in Figure 8.a, semi-analytical model and FE in Figure 8.b), whereas the real and imaginary parts are compared in Figure 8.c. The Table 3 presents the amplitude and the phase values obtained for the positions x=0mm and x=5mm. A good agreement (<3% in amplitude, <1° in phase) between simulated and experimental data is obtained for the position x=5mm. The discrepancy (24 % in amplitude, 1° in phase) observed at x=0mm for the calibration configuration is present again for the flaw configuration (24 % in amplitude, 2° in phase).

Flaw Signal

The signal of the flawed configuration is subtracted to the signal of the sane one to separate the signal due to the flaw over the one due to the borehole. In a fastened structure, boreholes do not perfectly duplicate, and this method cannot be used in industrial testing. Nevertheless, it gives an insight about the shape and the amplitude of the flaw response. Due to the small amplitude of the flaw signal (less than 1:4 mV, 10 times smaller than the borehole one) and due to the uncertainties of the experimental signal, the result of the flaw response is only compared to the FE result (Figure 8.d): the flaw signal has the same shape in the impedance plane, with a discrepancy in amplitude better than 30%.

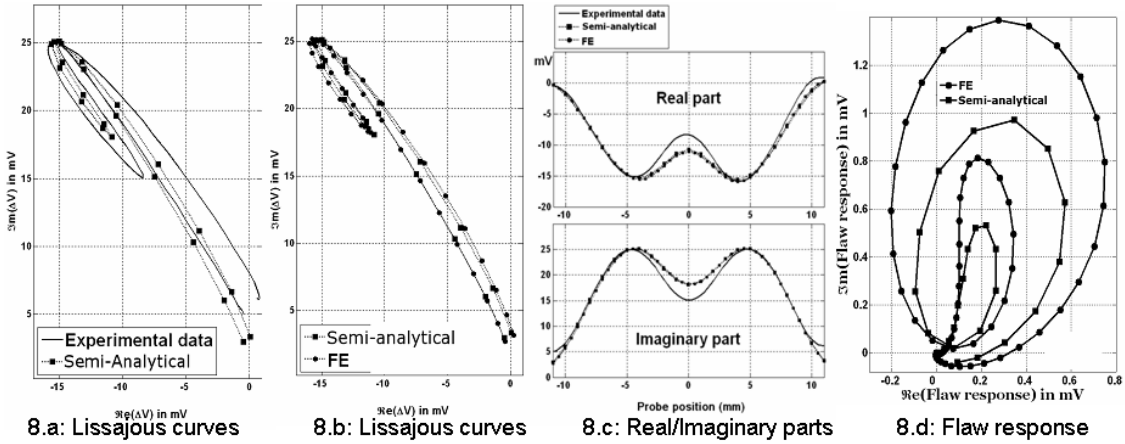

8.a: Lissajous curves 8.b: Lissajous curves 8.c: Real/Imaginary parts 8.d: Flaw response

Figure 8: Signals for the second layer flaw configuration.

Calibrated signals for the flawed borehole in the second layer		Measures		Agreements	
		Amplitude	Phase	Amplitude	Phase
Experiment	x= 0 mm	17 mV	119°	×	×
	x= 5 mm	29 mV	122°	×	×
CIVA	x= 0 mm	21 mV	121°	24 %	2°
	x= 5 mm	29 mV	121°	0%	1°
FE	x= 0 mm	21 mV	121°	24 %	2°
	x= 5 mm	30 mV	122°	3 %	0°

Table 3: Agreements between the signals for the second layer flaw configuration at 1.6kHz

6. Conclusions

This paper has presented recent progresses in developing models dedicated to Eddy Current testing. These codes, integrated in the CIVA platform, are based on semi-analytical approach to obtain fast and accurate results. Representative configurations of tube and flawed riveted structures ware illustrated, and obtained results show the good agreement between experimental and simulated data.

The future developments in CIVA will take into account the modeling of complex configurations (tube support plate, tubesheet, expanded part of steam generator tubes…) and the simulation of more realistic flaws (thin flaws, combination of different flaws…).

References

[1] Chew W.C, *Waves and Fields in Inhomogeneous Media*, Piscataway, IEEE Press (2nd edition), 1995.

[2] Prémel D, Pichenot G and Sollier T, "Development of a 3D electromagnetic model for eddy current tubing inspection", *International Journal of Applied Electromagnetics and Mechanics*, 2004 19 521-525.

[3] Harrington R.F, "The Method of Moments in Electromagnetics", *Journal of Electromagnetic Waves and Applications*, 1987 1 (3) 181–200.

[4] Auld B.A and Muennemann F.G and Riaziat M, *Nondestructive testing, Chapter 2: Quantitative modelling of flaw responses in eddy current testing*. vol. 7, London, Academic Press, 1984.

[5] Reboud C, Prémel D, Pichenot G, Lesselier D and Bisiaux B, "Development and validation of a 3D model dedicated to eddy current non destructive testing of tubes by encircling probes", *International Journal of Applied Electromagnetics and Mechanics*, 2007 25 313-317.

[6] Skarlatos A., Pichenot G., Lesselier D., Lambert M., Duchene B., Numerical modeling of EC non destructive evaluation of ferromagnetic tubes via an integral equation approach, progress in ENDE 2007.

[7] Paillard S., Pichenot G., Lambert M.,Voillaume H. and Dominguez N., A 3D model for eddy current inspection in aeronautics: application to riveted structures, Review of Progress in QNDE 26, 2006, pp. 265-272.

[8] Choua Y., Santandrea L., Le Bihan Y., Marchand C., Thin crack modeling in ECT with combined potential formulations.